ESTIMATION OF PLANT WATER CONTENT OF AGRICULTURAL CANOPIES USING HYPERSPECTRAL REMOTE SENSING

Catherine M. Champagne[a*], Karl Staenz[b], Abdou. Bannari[c], H. Peter White[b], Jean-Claude Deguise[b] and Heather McNairn[b]
[a]MIR Télédétection inc, 110 rue de la Barre (226), Longueuil, QC, Canada, J4K 1A3
[b]Canada Centre for Remote Sensing, Natural Resources Canada, 588 Booth St., Ottawa, ON, Canada K1A 0Y7
[c]Remote Sensing and Geomatics of Environment Laboratory, Department of Geography, University of Ottawa, P.O. Box 450, Stn. A, Ottawa (Canada), K1N 6N5
[*]corresponding author: catherine.champagne@ccrs.nrcan.gc.ca

Abstract

Hyperspectral models developed to estimate plant water content have had limited application under field conditions and have not been rigorously validated. A physical model using a spectrum matching technique was applied to hyperspectral data to directly calculate the canopy equivalent water thickness (EWT) using a look-up table approach. The objective of this study was to test the validity of this algorithm using plant water content information collected under field conditions, and to relate this to the needs of precision agriculture. Image data were acquired over two experimental test sites in Canada, near Clinton, Ontario and Indian Head, Saskatchewan, using the Probe-1 airborne hyperspectral sensor. Plant biomass samples were collected simultaneously from plots spanning fourteen fields of various crop types (wheat, canola, corn, beans and peas). The model was validated against EWT estimated from biomass samples. The model predicts EWT in the range found with all crop types pooled together, a root mean squared error (RMSE) of 26.8 % of the average. The model was sensitive to within-crop variability for broad leaf crops such as peas, corn, and beans (RMSE = 24.4%, 12.0, 21.8%, respectively).The RMSE for canola was relatively high (39.9%) as a result of a poor prediction at low water contents. The model proved a poor predictor of EWT in wheat (RMSE = 69.9%). EWT is related to plant biomass and leaf area index (LAI).

1 INTRODUCTION

The analysis of plant spectra measured from hyperspectral sensors using advanced models holds the potential to estimate plant physiological properties over relatively large areas. Reflectance in the near and short-wave infrared (NIR and SWIR, respectively) is influenced by the amount of liquid water in the target, expressed as a series of absorption features at 970, 1180, 1450, 1940 and 2500 nm. At the canopy scale, NIR bands have proven more sensitive to variation in plant water content due to the stronger reflectance signal.

The water index (WI), based on the relative depth of the 970 nm absorption feature, has been correlated with ground measures of plant water content at both leaf and canopy scales (Peñuelas *et al*., 1993; Gamon *et al*., 1999). The index has been found to be a good indicator of plant water stress (measured as relative water content) under extreme drought conditions where leaf area is not highly variable (Peñuelas *et al*., 1997). The WI is more strongly related to plant water content, which is a function of canopy biomass, than water stress, which is related to the physiological state of water in the plant (Gamon *et al*., 1999).

An increased understanding of the interaction of light within a plant canopy has led to more complex models to estimate plant water content. Reflectance in the NIR and SWIR are related to the overlapping absorption of atmospheric water vapour at 940 and 1130 nm and vegetation liquid water at 970 and 1180 nm. The absorption peak of liquid water is offset to longer wavelengths, corresponding to the larger intermolecular forces of water in this phase (Green *et al*., 1991). The transmission of radiation in these overlapping absorption bands is directly related to the total amount of water in each phase in a given pixel. Using a radiative transfer model, a curve fitting procedure was developed to estimate column atmospheric water vapour, and separate this amount from the liquid water (measured as equivalent water thickness, EWT) in the target vegetation, based on the offset in the absorption minima (Gao and Goetz, 1990).

The EWT is defined as the hypothetical thickness of a sheet of liquid water in the target (Allen

et al., 1969) and is related to the path length of light radiation in the canopy. Curve-fitting models have been applied using AVIRIS data over vegetated landscapes (Gao and Goetz, 1994; Roberts *et al.*, 1998; Ustin *et al.*, 1998) but have had limited application and validation over agricultural landscapes. The objective of this study is to validate this model using a version modified by Staenz et al. (1997) over an agricultural landscape and determine the sensitivity of this measure to within-field variation in plant water content.

2 MATERIALS AND METHODS

Airborne hyperspectral data and ground validation measures were collected over two agricultural sites in Canada representing a range of crop types and site characteristics. Field campaigns were conducted during the growing seasons near Clinton, Ontario (43°N, 81°W) in 1999 and Indian Head, Saskatchewan (50°N, 104°W) in 2000.

At the Clinton site, six test fields were chosen for ground validation measures, ranging in size from 19 to 36 hectares. Three were seeded with corn (*Zea mais L.*) and three with white beans (*Phaseolus vulgaris L.*). No nitrogen or seeding treatments were delineated within the fields.

For the Indian Head site, fields were located on a precision test farm of the Indian Head Agricultural Research Foundation. Eight 12-hectare fields were chosen for ground measurements, four seeded with wheat (*Triticum aestivum L.*), two seeded with canola (*Brassica napus L.*), and two with peas (*Lathyrus aphaca L.*). Each field was divided into four sections of approximately 3 hectares each to delimit treatments. Variable rate fertilizer applications were made in canola and wheat fields; variable rate seeding treatments were made in pea fields. Patches of bare soil, double seeded and crop residue were established in an adjacent field (approximately 20 m by 20 m in dimension).

2.1 Image Acquisition and Processing

Image data were acquired using the airborne Probe-1 hyperspectral sensor (Earth Search Sciences Inc., 2001). The Probe-1 is a "whiskbroom style" instrument that collects data in the cross-track direction by mechanical scanning and in the along-track direction by movement of the airborne platform. This sensor collects upwelling radiance in 128 spectral bands in the visible, NIR and SWIR between 440 nm and 2500 nm. The bandwidth is between 11 and 18 nm at full width half maximum (FWHM). Probe-1 is mounted on a three-axis gyrostabilizer to minimize geometric distortion from the aircraft movement. The flying altitude was 2500 m (above ground level) for a swath width of 3 km and a spatial resolution of 5 m at nadir.

Image processing was carried out using the Imaging Spectrometer Data Analysis System (ISDAS), a software package, developed at the Canada Centre for Remote Sensing, for processing and analysing hyperspectral data (Staenz *et al.*, 1998). A vicarious calibration of the sensor was required to correct for errors in the calibration coefficients supplied with the data (Secker *et al.*, 2001). A radiometric re-calibration of the sensor radiance was made using ground spectra obtained simultaneous to aircraft data acquisition over a pseudo-invariant site (bare soil in Clinton and a section of pavement in Indian Head), using a portable spectroradiometer (GER Corporation, 1990).

2.2 Calculation of Image EWT

Image data were used to calculate canopy equivalent water thickness using a spectral curve fitting procedure described by Staenz *et al.* (1997) and implemented in the ISDAS atmospheric correction module. The model calculates canopy EWT by modelling reflectance as a linear function adjusted for water absorption in the near infrared. An initial set of modelled surface reflectances was selected over the 940 nm atmospheric water absorption region and adjusted for liquid water transmittance. The adjusted surface reflectance was converted to at-sensor radiance using look-up table parameters derived using the MODTRAN 4 radiative transfer code (Berk *et al.*, 1999). The predicted at-sensor radiance was compared to the measured radiance using a non-linear least-squares fitting technique (Press, 1992). The model retrieves both the atmospheric water vapour content and the canopy liquid water on a pixel-by pixel-basis.

2.3 Ground Data Collection

Measurements of plant biomass used to calculate plant water content were made on the day of image acquisition for each study site. Approximately eight to thirteen sampling sites were selected per field. Sampling sites were selected to reflect within-field variability, based on elevation and soil maps, for a total of 154 locations. Each sampling site was georeferenced. At each sampling site, three replicates were taken within 2-3 m of the center of the site location to reflect local variation in plant biomass. At each replicate, all of the above-ground crop biomass was harvested within a 0.5 m by 0.5 m area. Samples were weighed and dried to obtain fresh and dry mass.

Plant EWT was calculated as (Jacquemoud and Baret, 1990):

$$EWT_{Biomass} = \frac{(FM - DM)}{LA}\ , \qquad (1)$$

where LA is the leaf area and FM and DM are the fresh and dry masses, respectively. The LA for this study was not measured directly, but was estimated from plant dry matter as:

$$LA = DM \times SLA\,, \qquad (2)$$

where SLA is the specific leaf area. The SLA is defined as the area of leaf per unit of dry leaf matter and is a crop-specific parameter that quantifies the internal structure of plant leaves, and is more or less constant for non-senescent leaves. For this experiment, indicative values were used from a table established by Keulen (1986).

The mass of water calculated was made on pooled samples of aboveground biomass, with no distinction made between stem and leaf water content. In general, leaves dominate the scattering of radiation within agricultural canopies (Knipling, 1970). The stem water content, however, is a significant portion of the total canopy biomass, particularly in the early stages of growth. For this reason, the values of biomass EWT were corrected for the stem-to-leaf ratio, to compensate for the effect of stem water content on these measures. The dry matter partitioning for agricultural crops is more strongly related to crop type than to individual growing conditions (Heemst, 1986). For this study, measured and modelled dry matter partition as a function of crop growth stage were estimated from studies on wheat (Schulze, 1982), corn (Heemst, 1986), soybean (Penning de Vries *et al*., 1989), canola (Hocking *et al*., 1997) and pea (Baigorri *et al*., 1999). Values for white bean were taken from soybean data due to the morphological similarities between these crops. Leaf proportions were estimated based on growth stage (days after sowing) and a correction factor (based on the mass) was applied to the total value of EWT.

2.4 Image Registration

Ground sampling sites were located in the Probe-1 image using an image-to-image registration with high-resolution georeferenced images (1 m IKONOS panchromatic for Indian Head sites and 1 m orthophotos for Clinton sites). The georeferenced image was warped to fit the Probe data using a 2nd order polynomial. Due to the high root mean squared error (average RMSE = 2.6 pixels) of the image registration, image data were averaged from 3 by 3-pixel window surrounding the georeferenced location.

2.5 Model Validation

To validate the model, the coefficient of determination and the root mean squared error (RMSE) were calculated. The RMSE and the standard deviation are given as a percentage of the average values. For this research, the observed values were those from the plant sampling ($EWT_{Biomass}$) and the predicted values were from the image (EWT_{Image}).

3 RESULTS

3.1 Model Validation

Model fit statistics were calculated for $EWT_{Biomass}$ values calculated both with and without stem water content for all crops combined (Table 1). The intercept for both cases is positive, indicating that the model is overestimating the amount of water in the canopy. This overestimation is reduced by 0.01 cm when the proportion of water attributable to stems is removed from the calculation of $EWT_{Biomass}$. The RMSE was much lower when biomass measures included the leaf water content only (26.8% versus 58.4%). This suggests that the model is more sensitive to leaf water content than the water content of the whole plant. This is advantageous for agricultural applications, where leaf water content responds more distinctly to drought conditions than the water content of the stem and leaves combined (Champagne *et al*., 2001).

There is a larger scatter in the data at values of EWT less than 0.15 cm. This is largely a result of the large scatter in the data for wheat fields, which will be discussed in section 3.3.

Table 2. *Fit statistics for observed EWT and image-derived EWT (where $EWT_{Biomass}$ and EWT_{Image} are the equivalent water thicknesses calculated from biomass samples and image data models; E_{Image} and $E_{Biomass}$ are the standard deviations as a percentage of the mean values; a and b are the slope and intercept of the least squares regression line; RMSE is the root mean squared error given as a percentage of the average value; D is the index of agreement; and R^2 the coefficient of determination, indicated in bold at significance level p< 0.001), given for the linear best fit line and a linear model fit through the bare soil point.*

	Case	$EWT_{Biomass}$ (cm)	EWT_{Image} (cm)	$E_{Biomass}$ (%)	E_{Image} (%)	*a*	*b*	*RMSE* (%)	R^2	R^2 (including bare soil point)
All Fields Combined	Stem + Leaves	0.191	0.142	55.4	40.8	0.8	0.06	58.4	**0.76**	
	Leaves Only	0.121	0.142	55.0	40.8	0.8	0.05	26.8	**0.76**	
Grouped by Crop Type (Leaves Only)	Bean	0.098	0.101	7.5	19.9	-0.1	0.13	21.8	0.01	0.11
	Corn	0.241	0.240	11.4	6.4	0.2	0.22	12.0	0.00	0.66
	Canola	0.101	0.131	57.0	38.2	0.9	0.06	39.6	**0.76**	**0.76**
	Pea	0.127	0.154	25.1	21.1	0.9	0.04	24.4	**0.74**	**0.81**
	Wheat	0.073	0.111	28.5	27.2	0.1	0.10	69.9	0.01	0.01

3.2 Background and geometric effects on modelled EWT

Image-derived measures such as EWT may be sensitive to variability that is related to differences in soil brightness or other background elements like crop residues. The early development phase of the crops and the minimum tillage used at both study sites resulted in a significant presence of crop residues and soil in the sensor field-of-view. Average EWT_{Image} values for patches of pure soil, and residue were examined. The bare soil patch had an EWT_{Image} value of 0.050 cm and the residue patch had a value of 0.007 cm. These values fall within the error bounds of the model, suggesting that soil and residue moisture did not contribute significantly to extracted EWT_{Image}.

The effects of view angle and illumination geometry on image-derived vegetation indices are significant (White *et al.*, 2001). For this study, image data were not normalized for directional effects, with most images acquired at approximately the same local sun time. Variations in view angle within a single image were not found to significantly influence the results. Future work will focus on the correction of errors due to variation in view/illumination geometry, since they have been found to cause some variation in estimated plant water content (White *et al.*, 2002).

3.3 Modelling crop and field variability

The dynamics of EWT as a measure of plant water content are further illustrated by examining the relationship between modelled and measured EWT on a species by species basis. Overall, the corn crop showed the highest EWT, with a decreasing EWT for peas, canola, wheat and beans (average EWT_{Image} = 0.240, 0.154, 0.131, 0.111, 0.010 cm, respectively). This follows the pattern of dry matter and water content distribution among the crop types (Fig. 1), confirming other studies that have found canopy

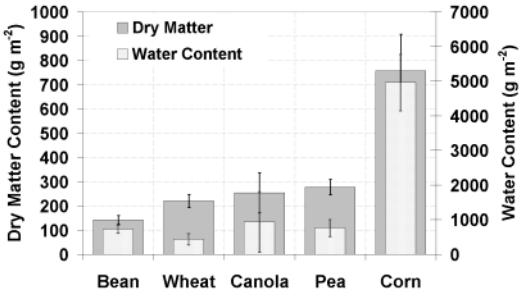

Fig. 1. *Dry matter and water content values for each crop type.*

estimates of plant water content largely driven by biomass distribution (Gamon *et al*, 1999).

A strong linear relationship was found for peas and canola, with R^2 values of 0.74 (significance level, $p = 0.001$) and 0.76 ($p = 0.001$), respectively (Table 1). The scatter plot of predicted and observed EWT shows that corn and bean crops were (with one exception) clumped within a limited range of EWT (Fig. 2), whereas the range of EWT for canola and peas was comparatively wider (57.0 % and 25. 1% variability, respectively). As a result of this limited dynamic range in corn and beans, R^2 values for these crops are low and not statistically significant. When R^2 values are recalculated using a bare soil point (with and EWT_{Image} value of 0.05cm and a $EWT_{Biomass}$ value of 0.0 cm, the relationship becomes stronger for corn ($R^2 = 0.66$). The relationship does not improve for beans substantially due to the very small range in $EWT_{Biomass}$ (7.5 %) compared to EWT_{Image} (19.9 %) for that crop. The linear fitting results for wheat were low despite a comparatively wider dynamic range of EWT in the data ($R^2 = 0.01$; $R^2 = 0.05$ including the bare soil point).

The RMSE for corn, bean, canola and pea crops was 12.0, 21.8, 39.6, and 24.4 % of the measured value, respectively. The higher RMSE for canola is largely a result of a poorer model fit. The predicted values are consistently higher than the measured values in this range of water values. This suggests that the ratio of stems to leaves for crops at this growth stage was not estimated correctly, or that the water content measured by the sensor includes a combination of both leaves and stems. Overall, the model is providing a good estimation of EWT for these crops.

The relationship between measured and modelled EWT for wheat showed the highest RMSE and the largest scatter in the data (Table 1, Fig. 1). The wheat crop showed significant variability within the four fields studied, with percentage variability of 28.5 % for $EWT_{Biomass}$ and 27.2 % for EWT_{Image}. The overall average water content was the lowest for the five crop types, with $EWT_{Biomass}$ of 0.073 cm. The RMSE was the highest for the five crops at 69.9%. The large scatter in the data suggests that the different radiation scattering regimes within the canopy for broadleaf and grass species influences the depth of water absorption features. It is possible that the erectophile nature of wheat leaves measured at a canopy scale produces an optical path length that

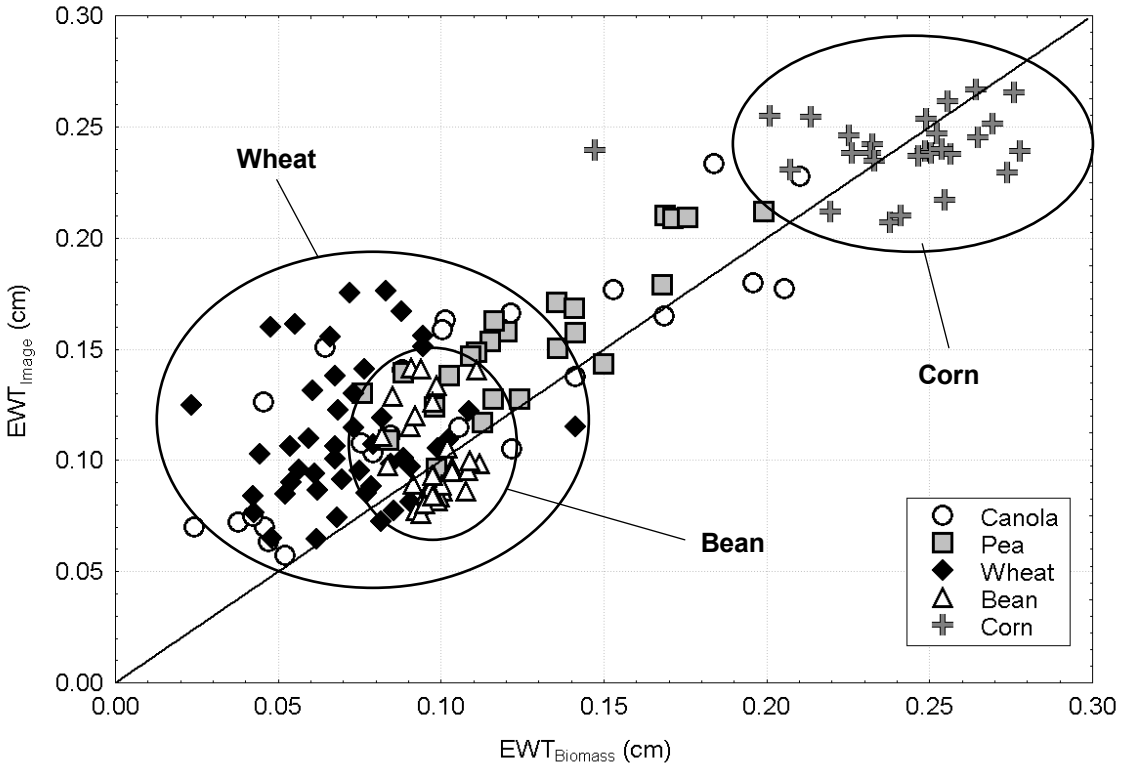

Fig. 2. *Relationship between EWT_{Image} and $EWT_{Biomass}$. Circled values represent clusters of data discussed in section 3.3.*

includes a highly variable proportion of leaves and stems, and that the EWT_{Image} values are not consistently representative of leaf or stem water content. Future work will establish the proportion of leaves and stems in the field-of-view of the sensor and will establish a mixing ratio to improve the understanding of plant parameters measured from airborne and satellite platforms.

3.4 Application of EWT to vegetation studies

The biological meaning of EWT must be understood in order for it to be an effective tool in vegetation studies. The canopy value of EWT used is related exponentially to the gravimetric water content of the plant (GWC_F), given as a percentage of the fresh mass (Fig.3). The relationship is slightly variable for each plant type, resulting from variability in specific leaf area and variation in the relationship between fresh and dry mass. The relationship is weak for EWT_{Image} ($R^2 = 0.24$) due to the large scatter in the EWT_{Image} values for beans. When beans are excluded from the model, the relationship improves ($R^2 = 0.64$).

EWT is primarily driven by changes in actual water content, which is, in turn, driven by changes in biomass. The EWT is related to NDVI ($R^2 = 0.77$), which is largely a measure of canopy structure and related to the total biomass through the leaf area index (LAI). This indicates that most of the variability in EWT is related to variation in canopy structure; primarily, increases in canopy height and LAI. The relationship between LAI and EWT is inherent: the EWT is a measure of the optical thickness of water in a stack of leaves; therefore increases in the quantity of leaves increases both the LAI and the EWT. Water thickness has been suggested to be a stronger indicator of canopy structure and LAI than indices, such as NDVI, which tend to saturate at LAI values greater than 3.0 (Roberts et al, 1998). The intercorrelation between physiological manifestations of water stress (such as stomatal closure) and variation in structural manifestations of water stress (such as variations in leaf water content) cannot be totally isolated from one another (Hsaio and Bradford, 1983). Optical measures of plant water content, in an agricultural context, can instead form part of an integrated approach to crop management (Strachan *et al*., 2001).

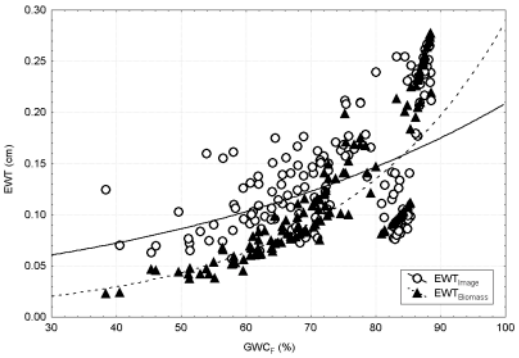

Fig. 3. *Relationship between gravimetric water content (GWC_F) and EWT calculated from biomass and image data. Lines indicate a best-fit exponential model for $EWT_{Biomass}$ ($R^2 = 0.85$) and EWT_{Image} ($R^2 = 0.24$).*

4 CONCLUSIONS

A spectrum-matching technique for the prediction of canopy water was validated over an agricultural landscape. Overall, the model provides a significant relationship with canopy equivalent water thickness (EWT) when all crop types are pooled together, with an RMSE of 26.8%. The model is more sensitive to leaf water content than plant water content, and future validation work should isolate these values in the biomass measurements.

A breakdown of the estimation of EWT for individual crops revealed that the sensitivity of the model to variations in EWT. The model was sensitive to the high variability pea crops (24.4%) and provided a good prediction of EWT in canola at higher water conent (RMSE = 39.9%). The low level of variability in corn and bean crops prevented a statistically significant result from being found, but the low RMSE suggests that the model accurately estimated EWT for these crops (RMSE = 12.0 and 21.8% for corn and beans, respectively). The application of this model to agricultural field management would require a greater understanding of the causes of variation in EWT and the link to crop production. The poor results for wheat (RMSE = 69.9%) suggest that the source of scattering of radiation from these canopies is a variable combination of leaves and stems. The influence of stems in grass species reflectance should be examined further.

The relationship of EWT to LAI ($R^2 = 0.67$) makes it a useful tool to use in conjunction with other remote sensing measures for an integrated system of crop management.

Future work will be done to examine measures of EWT in relation to precision agriculture. A follow-up study was made in 2002 at Indian Head to examine seasonal variation in optical remote sensing products such as EWT. Two wheat fields were studied during three field campaigns over the growing season. Leaf-level spectral measurements were made at each sampling site, coincident with biomass sampling. Hyperion hyperspectral satellite imagery was acquired over the site to examine potential to scale-up the estimation of water content to space-borne platforms.

Acknowledgements

This research was carried out as part of a master's thesis project at the University of Ottawa and the authors wish to thank them for financial support through the Natural Sciences and Engineering Research Council (NSERC). The authors gratefully acknowledge all participants in the Clinton and Indian Head field campaigns.

REFERENCES

[1] Allen, W.A., H.W. Gausman, A.J. Richardson, and J.R. Thomas, 1969, Interaction of isotropic light with a compact leaf, *Journal of the Optical Society of America*, **58(8)**, 1023-1028.

[2] Baigorri, H., M.C. Antolín, and M. Sánchez-Díaz, 1999. Reproductive response of two morphologically different pea cultivars to drought, *European Journal of Agronomy*, **10**, 119-128.

[3] Berk, A., G.P. Anderson, P.K. Acharya, J.H. Chetwynd, L.S. Bernstein, E.P. Shettle, M.W. Matthew, and S.M. Adler-Golden, 1999, *MODTRAN 4 User's Manual*, Air Force Research Laboratory, Hanscom AFB, Maryland, U.S.A.

[4] Champagne, C., E. Pattey, A. Bannari, and I.B. Strachan, 2001, Mapping crop water status: issues of scale in the detection of crop water stress using hyperspectral indices, Proceedings of the 8th International Symposium on Physical Measurements and Signatures in Remote Sensing, Aussois, France, pp.79-84.

[5] Earth Search Sciences Inc., 2001, About Probe-1, Kalispell,MT., www.earthsearch.com/technology.

[6] Gamon, J.A., H.-L. Qiu, D.A. Roberts, S.L. Ustin, D.A. Fuentes, A. Rahman, D. Sims, and C. Stylinski, 1999, Water expressions from hyerpspectral reflectance: implications for ecosystem flux modeling. Proceedings of the Eigth Annual Airborne Visible/Infrared Imaging Spectrometer (AVIRIS) Workshop, Pasadena, CA, JPL Publication, cd-rom.

[7] Gao, B.-C., and A.F.H. Goetz, 1990, Column atmospheric water vapor and vegetation liquid water retrieval from Airborne Imaging Spectrometer data, *Journal of Geophysical Research*, **95**, 3549-3564.

[8] Gao, B.-C., and A.F.H. Goetz, 1994, Extraction of dry leaf spectral features from reflectance spectra of green vegetation, *Remote Sensing of Environment*, **47**, 369-374.

[9] Geophysical and Environmental Research Corporation, 1990, GER 3700 *Spectroradiometer User's Manual*, v.2.1, 55 pages.

[10] Green, R.O., J.E. Conel, J.S. Margolis, C.J. Brugge, and G.L. Hoover, 1991, An inversion algorithm for the retrieval of atmospheric and leaf water absorption from AVIRIS radiance with compensation for atmospheric scattering, Proceedings of the Third Annual Airborne Visible/Infrared Imaging Spectrometer (AVIRIS) Workshop, Pasadena, California, JPL Publication 91-28, pp.51-61.

[11] Heemst, H.D.J. van., 1986, Crop phenology and dry matter distribution, in Modelling of Agricultural Production, H. van Keulen and J. Wolf (eds), pp. 26-38.

[12] Hocking, P.J., P.J. Randall, and D. DeMarco, 1997, The response of dryland canola to nitrogen fertilizer: partitioning and mobilization of dry matter and nitrogen, and nitrogen effects on yield components, *Field Crops Research*, **54**, 201-220.

[13] Hsiao, T. C., and K. J. Bradford. 1983, Physiological consequences of cellular water deficits, Chapter 6A. *Limitations to Efficient Water Use in Crop Production*, edited by H. M. Taylor, W.R. Jordan, and T. R. Sinclair (eds.), American Society of Agronomy, Madison, WI. pp. 227-265.

[14] Jacquemoud, S., and Baret F, 1990, PROSPECT: a model of leaf optical properties spectra, *Remote Sensing of Environment*, **34**, 75-91.

[15] Keulen, H. van., 1986, Plant data, in *Modelling of Agricultural Production*, edited by H. van Keulen and J. Wolf, pp. 235-247.

[16] Knipling, E.B., 1970. Physical and physiological basis for the reflectance of visible and near infrared radiation from vegetation, *Remote Sensing of Environment*, **1**, 155-159.

[17] Penning de Vries, F.W.T., D.M. Jansen, H.F.M. ten Berge, and A. Bakema, 1989, *Simulation of Ecophyiological Processes in Several Annual Crops*, Purdoc: Wageningen, 332 pages.

[18] Peñuelas, J., I. Filella, C. Biel, L. Serrano, and R. Savé, 1993, The reflectance at the 950-970 region as an indicator of plant water status, *International Journal of Remote Sensing*, **14(10)**, 1887-1905.

[19] Peñuelas, J., J. Piñol, R. Ogaya, and I. Filella, 1997, Estimation of plant water concentration by the reflectance water index WI (R900/R970), International Journal of Remote Sensing, **18(13)**, 2869-2875.

[20] Press, W.H., S.A. Teulkosky, W.T. Vetterling, and B.P. Flannery, 1992, *Numerical Recipes in C*, Cambridge University Press, Cambridge, England, 994 pages.

[21] Roberts, D.A., K. Brown, R. Green, S. Ustin, and T. Hinckley, 1998, Investigating the relationship

between liquid water and leaf area in clonal populus, Summaries of the Seventh JPL Earth Science Workshop held in Pasadena, CA, cd-rom

[22] Schulze, E.-D. 1982. Plant Life Forms and Their Carbon, Water and Nutrient Relations, in *Physiological Plant Ecology II*, edited by O.L. Lange, P.S. Nobel, C.B. Osmond and H. Ziegler, pp. 615-667.

[23] Secker, J., K. Staenz, R.P. Gauthier, and P. Budkewitsch, 2001; Vicarious calibration of airborne hyperspectral sensors in operational environments, *Remote Sensing of Environment*, **76**, 81-92.

[24] Staenz, K., and T. Szeredi, R.J. Brown, H. McNairn, and R. Van Acker, 1997, Hyperspectral information extraction techniques applied to agricultural casi data for detection of within field variations, in Proceedings of the International Symposium, Geomatics in the Era of RADARSAT (GER'97) held in Ottawa, Canada, cd-rom.

[25] Staenz, K., T. Szeredi, and J. Schwarz, 1998. ISDAS- A system for processing/analyzing hyperspectral data, *Canadian Journal of Remote Sensing*, **42(2),** 99-113.

[26] Strahan, I.B., E. Pattey, J. Boisvert, and J. Daoust, 2001, Impact of nitrogen and environmental conditions on corn as detected by hyperspectral reflectance, *Remote Sensing of Environment*, **80,** 213-224**.**

[27] Ustin, S.L. and D.A. Roberts, J. Pinzón, S. Jacquemoud, M. Gardner, G. Scheer, C.M. Castañeda and A. Palacios-Orueta, 1998, Estimating canopy water content of chaparral shrubs using optical methods, *Remote Sensing of Environment*, **65**,280-291.

[28] White, H.P., J.R. Miller, and J.M Chen, Four-scale linear model for anisotropic reflectance (FLAIR) for plant canopies. I: Model description and partial validation. *IEEE Transactions on Geoscience and Remote Sensing*, **39(5)**, 1072-1083.

[29] White H. P. , Sun L. , Champagne C. , Staenz K. , Leblanc S. G., 2002, BRDF Normalization of Hyperspectral Image Data, IGARSS 2002, held at Toronto, Canada, June 24-28 , 2002.